Research in Astron. Astrophys. **2011** Vol. **11** No. **3**, 353–368
*http://www.raa-journal.org* *http://www.iop.org/journals/raa*

*Research in Astronomy and Astrophysics*

# Symplectic integrators with potential derivatives to third order *

Wei Sun, Xin Wu and Guo-Qing Huang

Institute of Astronomy & Department of Physics, Nanchang University, Nanchang 330031, China; *xwu@ncu.edu.cn*

Received 2010 August 4; accepted 2010 October 25

**Abstract** An operator associated with third-order potential derivatives and a force gradient operator corresponding to second-order potential derivatives are used together to design a number of new fourth-order explicit symplectic integrators for the natural splitting of a Hamiltonian into both the kinetic energy with a quadratic form of momenta and the potential energy as a function of position coordinates. Numerical simulations show that some new optimal symplectic algorithms are much better than their non-optimal counterparts in terms of accuracy of energy and position calculations.

**Key words:** celestial mechanics — methods: numerical

## 1 INTRODUCTION

Complicated dynamical behaviors in celestial mechanics bring computational challenges. It is necessary to have good orbit determinations. Geometric integrators such as manifold correction schemes and symplectic methods are confirmed to yield a substantially improved long-term behavior compared to classical integrators like Runge-Kutta algorithms. The manifold correction schemes mean the preservation of some invariant manifolds in every integration step of the classical integrators used (Wu et al. 2007; Ma et al. 2008; Zhong & Wu 2010), and the symplectic methods deal with symplectic structure-preservation algorithms designed specifically for a Hamiltonian dynamical system. Seen from the perspective of qualitative research, the structure-preservation becomes more important than the manifold-preservation. Because of this, the development and application of symplectic methods are considered here.

There are two kinds of symplectic integration algorithms. One is implicit symplectic integrators for an inseparable Hamiltonian system (Feng 1985, 1986), and the other is explicit symplectic integrators for a separable Hamiltonian system. As an illustration, there seem to be a third kind of symplectic method obtained from a combination of the two types (Liao 1997; Preto & Saha 2009; Lubich et al. 2010; Zhong et al. 2010). In essence, they are mainly regarded as the first type, namely, implicit *splitting* integrators. Thanks to an advantage for convenience of application, the explicit symplectic integrators have become widely popular in a number of references. When a Hamiltonian system can naturally be split into two integrable parts of kinetic and potential energies, the explicit second- and third-order symplectic algorithms were built by Ruth (1983). Then, there were the fourth-order symplectic integrators (Forest & Ruth 1990), and higher-order symplectic schemes by the composition method of Yoshida (1990). These are attributed to the usual non-gradient symplectic

* Supported by the National Natural Science Foundation of China.

algorithms. A notable point is that the third-order force gradient symplectic integrator was present when the usual third-order symplectic integrator began to appear in the literature. By the included force gradient operator, fourth-order force gradient symplectic algorithms were developed (Chin 1997, 2007; Omelyan et al. 2002). It was reported that these gradient methods are more accurate than their corresponding usual non-gradient ones. Recently, it has been shown that the optimal third-order gradient symplectic methods with the norm of fourth-order truncation errors being minimized are better than the non-optimal ones in terms of the quality of integration, even typically superior to the usual fourth-order symplectic integrators of Forest & Ruth (Li & Wu 2010a, b). In addition, the fourth-order force gradient symplectic integrators are extended to solve a gravitational $n$-body Hamiltonian separated into a dominant Keplerian part and a perturbation in Jacobi coordinates (Xu & Wu 2010). Of course, the most popular usual symplectic integrator for the Hamiltonian decomposition is the second-order leapfrog symplectic scheme, first introduced by Wisdom & Holman (1991). Along this idea, the symplectic correctors (Wisdom et al. 1996) and the pseudo-high-order symplectic integrators (Chambers & Murison 2000), as optimized algorithms, were proposed.

It should be emphasized that the force gradient operator mentioned above depends on the second-order potential derivatives. Another operator associated with the third-order potential derivatives will be found to be easy in practical computations. Based on Yoshida's composition method by the two included operators, a class of new high-order explicit symplectic integrators for the natural splitting of a Hamiltonian should be constructed from a theoretical point of view. This is our main motivation in the present paper. Therefore, in Section 2 we provide the new fourth-order explicit symplectic integrators including optimized algorithms with the least norm of fifth-order truncation errors. Then, they are evaluated through a series of numerical simulations in Section 3. Finally, Section 4 gives our conclusions.

## 2 CONSTRUCTION OF NEW SYMPLECTIC ALGORITHMS

Some notations are introduced here. Let $\boldsymbol{p}$ and $\boldsymbol{q}$ be momentum and coordinate vectors, respectively. Their $i$th components are $p_i$ and $q_i$. For a separable Hamiltonian system

$$H = T + V, \tag{1}$$

two Lie derivatives with respect to the kinetic energy $T = \boldsymbol{p}^2/2$ and the potential energy $V = V(\boldsymbol{q})$ are specified as

$$A = \{\ , T\} = \sum_i p_i \frac{\partial}{\partial q_i}, \qquad B = \{\ , V\} = \sum_i F_i \frac{\partial}{\partial p_i}, \tag{2}$$

where force $F_i = -\partial V/\partial q_i = -V_i$, and the symbol $\{,\}$ denotes the Poisson bracket. If commutator $[A, B] = AB - BA$ is given, then it is easy to work out the commutator $[B, [A, B]]$ (Xu & Wu 2010)

$$\begin{aligned} C &= [B,[A,B]] = \{\ ,\{V,\{T,V\}\}\} = 2\sum_i\sum_j\sum_k V_{ij}V_kT_{jk}\frac{\partial}{\partial p_i} \\ &= 2\sum_i\sum_j F_j\frac{\partial F_i}{\partial q_j}\frac{\partial}{\partial p_i} = 2\sum_i\sum_j F_j\frac{\partial F_j}{\partial q_i}\frac{\partial}{\partial p_i} = \sum_i \nabla_i|\boldsymbol{F}|^2\frac{\partial}{\partial p_i} \end{aligned} \tag{3}$$

with $V_{ij} = \partial^2 V/\partial q_i\partial q_j$ and $T_{jk} = \partial^2 T/\partial p_j\partial p_k = \delta_{jk}$. This sufficiently shows that $C$ is simply the gradient of the square of the force, $\boldsymbol{F}\cdot\boldsymbol{F}$. In this sense, $C$ is called the force gradient operator connected with the first- and second-order potential derivatives. Further, we can calculate a more complicated commutator in the following manner

$$\begin{aligned} D &= [B,[A,[B,[A,B]]]] = \{\ ,\{V,\{T,\{V,\{T,V\}\}\}\}\} \\ &= -2\sum_i\sum_j\sum_k V_k(2V_{jk}V_{ij} + V_jV_{ijk})\frac{\partial}{\partial p_i}, \end{aligned} \tag{4}$$

where $V_{ijk} = \partial^3 V/\partial q_i \partial q_j \partial q_k$. That is to say, $D$ is an operator associated with the first-, second- and third-order potential derivatives. It is worth noting that $A$ and anyone of $B$ ($C$ or $D$) represent two different types of operators. Clearly, the Lie derivatives of the momenta via $A$ are always identical to zero. So are the ones with respect to the positions by $B$, $C$ or $D$. Equivalently, $Ap_i = Bq_i = Cq_i = Dq_i \equiv 0$. In other words, $A$ is a position-type operator which affects the dominant evolution of the positions, and any combination of $B$, $C$ or $D$ represents the momentum-type operator which affects the evolution of the momenta. However, $[B,[B,[B,[B,A]]]] = [A,[B,[B,[B,A]]]] \equiv 0$ for any position and momentum.

The common symplectic integrators such as those of Yoshida (1990) are taken from symmetric compositions of the two operators $A$ and $B$. When the operator $C$ is added to these compositions, the so-called force gradient symplectic integrators are obtained (Chin 1997, 2007; Omelyan et al. 2002). Now, we use the four operators $A$, $B$, $C$ and $D$ to establish new symplectic integrators from the two different compositions.

### 2.1 Position Type Algorithms Containing $D$ at the Midpoint of Compositions

Let us begin with the following symmetric combinatorial products of exponential functions of Lie operators

$$\begin{aligned}(\mathrm{A}) \quad \exp(W) \;=\; & \exp(a\tau A)\otimes\exp(b\tau B + c\tau^3 C)\otimes\exp(d\tau A)\otimes\exp(e\tau B + f\tau^3 C + g\tau^5 D)\\ & \otimes\exp(d\tau A)\otimes\exp(b\tau B + c\tau^3 C)\otimes\exp(a\tau A),\end{aligned} \tag{5}$$

where $\tau$ stands for a step size, and unknown time coefficients $a, b, c, d, e, f$ and $g$ need to be determined. Based on the Baker-Campbell-Hausdorff (BCH) formula, $W$ is given by the expansion

$$\begin{aligned}W \;=\; & (\alpha_1 A + \alpha_2 B)\tau + (\beta_1[B,[A,B]] + \beta_2[A,[A,B]])\tau^3 + (\gamma_1[A,[A,[B,[A,B]]]]\\ & +\gamma_2[A,[A,[A,[A,B]]]] + \gamma_3[B,[A,[A,[A,B]]]] + \gamma_4 D)\tau^5 + \mathcal{O}(\tau^7).\end{aligned} \tag{6}$$

In the above equation, $\alpha_1, \alpha_2, \beta_1, \beta_2, \gamma_1, \gamma_2, \gamma_3$ and $\gamma_4$ read

$$\begin{aligned}
\alpha_1 \;&=\; 2(a+d),\\
\alpha_2 \;&=\; e+2b,\\
\beta_1 \;&=\; 2c + f - \frac{1}{6}de^2 + \frac{1}{3}deb + \frac{1}{3}db^2 - \frac{1}{6}a(e+2b)^2,\\
\beta_2 \;&=\; \frac{2}{3}d^2 b - \frac{1}{6}d^2 e - \frac{1}{3}da(e+2b) - \frac{1}{6}a^2(e+2b),\\
\gamma_1 \;&=\; -\frac{1}{6}d^2 f + \frac{1}{60}d^3 e^2 + \frac{2}{3}d^2 c + \frac{1}{15}d^3 eb - \frac{8}{30}d^3 b^2\\
&\quad -\frac{1}{3}da\Big(2c + f - \frac{1}{6}de^2 + \frac{1}{3}deb + \frac{1}{3}db^2\Big) + \frac{1}{6}a(e+2b)\Big(\frac{2}{3}d^2 b - \frac{1}{6}d^2 e\Big)\\
&\quad -\frac{1}{6}a^2\Big(2c + f - \frac{1}{6}de^2 + \frac{1}{3}deb + \frac{1}{3}db^2\Big) + \Big(\frac{8}{360}d^2 a - \frac{4}{90}da^2 + \frac{1}{60}a^3 + \frac{2}{30}da^2\Big)(e+2b)^2,\\
\gamma_2 \;&=\; \frac{7}{360}d^4 e - \frac{16}{360}d^4 b - \Big(\frac{1}{3}da + \frac{1}{6}a^2\Big)\Big(\frac{2}{3}d^2 b - \frac{1}{6}d^2 e\Big)\\
&\quad +\Big(\frac{7}{360}a^4 + \frac{8}{360}d^3 a + \frac{8}{90}d^2 a^2 + \frac{7}{90}da^3\Big)(e+2b),\\
\gamma_3 \;&=\; \frac{1}{45}d^3 e^2 - \frac{7}{90}d^3 eb + \frac{8}{90}d^3 b^2 - \frac{1}{3}a(e+2b)\Big(\frac{2}{3}d^2 b - \frac{1}{6}d^2 e\Big)\\
&\quad +\Big(\frac{4}{360}d^2 a + \frac{2}{30}da^2\Big)(e+2b)^2 + \frac{1}{45}a^3(e+2b)^2,
\end{aligned}$$

$$\begin{aligned}\gamma_4 \;=\; & g-\frac{1}{3}def+\frac{1}{30}d^2e^3+\frac{1}{3}dec+\frac{1}{3}dbf-\frac{1}{20}d^2e^2b-\frac{1}{60}d^2eb^2\\ & +\frac{2}{3}dcb-\frac{1}{15}d^2b^3-\frac{1}{3}a(e+2b)\Big(2c+f-\frac{1}{6}de^2-\frac{1}{3}deb-\frac{1}{3}db^2\Big)\\ & +\frac{4}{360}da(e+2b)^3+\frac{1}{30}a^2(e+2b)^3. \end{aligned} \tag{7}$$

Obviously, fourth-order conditions must satisfy four relations

$$\alpha_1=1,\quad \alpha_2=1,\quad \beta_1=\beta_2=0. \tag{8}$$

Besides those, an additional constraint on $D$ (i.e. $\gamma_4 = 0$) in the $\mathcal{O}(\tau^5)$ terms representing the truncation errors should be given by

$$\begin{aligned} g \;=\; & \frac{1}{3}def-\frac{1}{30}d^2e^3-\frac{1}{3}dec-\frac{1}{3}dbf+\frac{1}{20}d^2e^2b+\frac{1}{60}d^2eb^2\\ & -\frac{2}{3}dcb+\frac{1}{15}d^2b^3+\frac{1}{3}a(e+2b)\left(2c+f-\frac{1}{6}de^2+\frac{1}{3}deb+\frac{1}{3}db^2\right)\\ & -\frac{4}{360}da(e+2b)^3-\frac{1}{30}a^2(e+2b)^3. \end{aligned} \tag{9}$$

In terms of Equations (8) and (9), we have

$$\begin{aligned} a \;&=\; \frac{1}{2}-d,\\ b \;&=\; \frac{1}{24d^2},\\ e \;&=\; 1-\frac{1}{12d^2},\\ f \;&=\; \frac{1}{12}-\frac{1}{24d}+\frac{1}{576d^3}-2c,\\ g \;&=\; \frac{c}{12d}+\frac{1}{768d^2}+\frac{1}{480}-cd-\frac{1}{288d}-\frac{1}{27648d^4}, \end{aligned}$$

and the coefficients of the truncation errors

$$\begin{aligned} \gamma_1 \;&=\; cd^2-\frac{1}{1152d}+\frac{1}{480},\\ \gamma_2 \;&=\; \frac{d^2}{288}-\frac{1}{1920},\\ \gamma_3 \;&=\; \frac{d}{144}+\frac{1}{1728d}-\frac{1}{240}. \end{aligned}$$

Due to the existence of the two free parameters $c$ and $d$, there are an infinite number of fourth-order integrators from a theoretical point of view. Of course, the choice of $c$ and $d$ has an effect on the norm of the fifth-order truncation errors

$$\gamma=\sqrt{\gamma_1^2+\gamma_2^2+\gamma_3^2}. \tag{10}$$

In the following, some fourth-order symplectic integrators are listed according to several possible values of $\gamma$.

**Case 1:** optimization of the norm $\gamma$ with respect to the two time coefficients $c$ and $d$. — A necessary condition for obtaining the minimized norm $\gamma_{\min}$ is

$$\frac{\partial\gamma}{\partial c}=\frac{\partial\gamma}{\partial d}=0. \tag{11}$$

Taking into account Equations (8), (9) and (11), we can arrive at the global minimum of the norm $\gamma_{\min} \approx 1.13\,\text{e–5}$ when the time coefficients are determined by

$$\begin{aligned}(\text{A1})\quad a &= 0.115859581211902\,\text{e+0}, & b &= 0.282363624036460\,\text{e+0},\\ c &= 1.195426044501562\,\text{e–3}, & d &= 0.384140418788098\,\text{e+0},\\ e &= 0.435272751927079\,\text{e+0}, & f &= 3.102414949088467\,\text{e–3},\\ g &= 7.348945247751502\,\text{e–6}.\end{aligned} \tag{12}$$

**Case 2:** optimization of the norm $\gamma$ with respect to one of the two time coefficients $c$ and $d$. — Let us suppose $c$ is a free parameter. At once, $d$ can be solved from the minimum norm $\gamma_{\min}$. This means that there is a problem of how to find the minimization of $\gamma$ versus one time coefficient $d$. For example, setting $c = 1.353\,\text{e–3}$, we have $\gamma_{\min} \approx 1.66\,\text{e–5}$ if the other time coefficients satisfy

$$\begin{aligned}(\text{A2})\quad a &= 0.118829530397266\,\text{e+0}, & b &= 0.286780926768790\,\text{e+0},\\ d &= 0.381170469602734\,\text{e+0}, & e &= 0.426438146462420\,\text{e+0},\\ f &= 2.663630070575213\,\text{e–3}, & g &= 2.542599508647495\,\text{e–6}.\end{aligned} \tag{13}$$

In addition, for $c = 0$ we obtain $\gamma_{\min} \approx 2.13\,\text{e–4}$ with

$$\begin{aligned}(\text{A3})\quad a &= 7.031087134179426\,\text{e–2}, & b &= 0.225673220373456\,\text{e+0},\\ d &= 0.429689128658206\,\text{e+0}, & e &= 0.548653559253087\,\text{e+0},\\ f &= 8.247384758086507\,\text{e–3}, & g &= -6.164365178933876\,\text{e–6}.\end{aligned} \tag{14}$$

Of course, $d$ can also be viewed as a free parameter. Thus, $c$ can be given by the minimum norm $\gamma_{\min}$. For instance, when $d = 0.3769$ we should require

$$\begin{aligned}(\text{A4})\quad a &= 0.1231\,\text{e+0}, & b &= 0.293316492742892\,\text{e+0},\\ c &= 1.547389121085482\,\text{e–3}, & e &= 0.413367014514215\,\text{e+0},\\ f &= 2.113996492826425\,\text{e–3}, & g &= 3.424612994889793\,\text{e–6}\end{aligned} \tag{15}$$

so as to get $\gamma_{\min} \approx 3.09\,\text{e–5}$.

**Case 3:** non-optimization. — If $f = 0$ and $c = 0$, we have $\gamma \approx 1.12\,\text{e–2}$ and

$$\begin{aligned}(\text{A5})\quad a &= +0.675603595979829\,\text{e+0}, & b &= +1.35120719195966\,\text{e+0},\\ d &= -0.175603595979829\,\text{e+0}, & e &= -1.70241438391932\,\text{e+0},\\ g &= +2.604494332549321\,\text{e–2}.\end{aligned} \tag{16}$$

When $c = 0.3$ and $d = 0.1$, it is easy to get $a = 0.4$, and the other coefficients become

$$\begin{aligned}(\text{A6})\quad b &= +4.16666666666667\,\text{e+0}, & e &= -7.333333333333333\,\text{e+0},\\ f &= +8.02777777777777\,\text{e–1}, & g &= -4.412037037037036\,\text{e–2},\end{aligned} \tag{17}$$

and the norm $\gamma \approx 4.31\,\text{e–3}$.

As a special case, when $c = f = g = 0$ Equation (5) is just the usual fourth-order non-gradient symplectic algorithm (Forest & Ruth 1990) with

$$\begin{aligned}(\text{FR})\quad a &= \frac{1}{2}b, & b &= \frac{1}{2-\sqrt[3]{2}},\\ d &= \frac{1}{2}(1-b), & e &= 1-2b.\end{aligned} \tag{18}$$

In addition, at $e = f = g = 0$ Equation (5) becomes the force gradient fourth-order symplectic scheme (Chin 1997) with

$$\begin{aligned} \text{(Ch)} \quad a &= \frac{1}{2}(1-\frac{1}{\sqrt{3}}), & b &= \frac{1}{2}, \\ c &= \frac{1}{48}(2-\sqrt{3}), & d &= \frac{1}{2\sqrt{3}}. \end{aligned} \tag{19}$$

### 2.2 Momentum Type Algorithms with $D$ at the Ends of Compositions

By exchanging the position type operator $A$ with the momentum type operators $B$, $C$ or $D$, another kind of composition is written as

$$\begin{aligned} \text{(B)} \quad \exp(W) &= \exp(a\tau B + b\tau^3 C + g\tau^5 D) \otimes \exp(c\tau A) \otimes \exp(d\tau B + e\tau^3 C) \otimes \exp(f\tau A) \\ &\quad \otimes \exp(d\tau B + e\tau^3 C) \otimes \exp(c\tau A) \otimes \exp(a\tau B + b\tau^3 C + g\tau^5 D). \end{aligned} \tag{20}$$

In the same way as mentioned above, we obtain

$$\begin{aligned} W &= (\alpha_1 A + \alpha_2 B)\tau + (\beta_1[B,[A,B]] + \beta_2[A,[A,B]])\tau^3 + (\gamma_1[A,[A,[B,[A,B]]]] \\ &\quad + \gamma_2[A,[A,[A,[A,B]]]] + \gamma_3[B,[A,[A,[A,B]]]] + \gamma_4 D)\tau^5 + \mathcal{O}(\tau^7), \end{aligned} \tag{21}$$

where

$$\begin{aligned} \alpha_1 &= 2c + f, \\ \alpha_2 &= 2(a+d), \\ \beta_1 &= 2b + 2e + \frac{1}{6}d^2 f - \frac{2}{3}cd^2 + \frac{1}{3}ad(2c+f) + \frac{1}{6}a^2(2c+f), \\ \beta_2 &= \frac{1}{6}df^2 - \frac{1}{3}cdf - \frac{1}{3}c^2 d + \frac{1}{6}a(2c+f)^2, \\ \gamma_1 &= \frac{1}{6}ef^2 - \frac{1}{30}d^2 f^3 - \frac{1}{3}cef - \frac{1}{3}c^2 e + \frac{4}{60}c^3 d^2 + \frac{1}{20}cd^2 f^3 + \frac{1}{60}c^2 d^2 f + \frac{1}{6}b(2c+f)^2 \\ &\quad - \frac{1}{3}a(2c+f)\Big(\frac{1}{6}df^2 - \frac{1}{3}cdf - \frac{1}{3}c^2 d\Big) - \Big(\frac{4}{360}ad + \frac{1}{30}a^2\Big)(2c+f)^3, \\ \gamma_2 &= \frac{14}{360}c^4 d - \frac{1}{360}df^4 - \frac{8}{360}cdf^3 + \frac{1}{60}c^2 df^2 + \frac{7}{90}c^3 df - \frac{1}{360}a(2c+f)^4, \\ \gamma_3 &= \frac{1}{90}d^2 f^3 - \frac{1}{10}cd^2 f^2 + \frac{4}{45}c^3 d^2 + \frac{4}{30}c^2 d^2 f + \frac{1}{6}a(2c+f)\Big(\frac{1}{6}df^2 - \frac{1}{3}cdf - \frac{1}{3}c^2 d\Big) \\ &\quad + \Big(\frac{1}{90}a^2 - \frac{2}{360}ad\Big)(2c+f)^3, \\ \gamma_4 &= 2g + \frac{1}{3}def - \frac{1}{60}d^3 f^2 - \frac{4}{3}cde - \frac{1}{15}cd^3 f + \frac{8}{30}c^2 d^3 + \frac{1}{3}bd(2c+f) \\ &\quad + \frac{1}{6}a(2c+f)(2e + \frac{1}{6}d^2 f - \frac{2}{3}cd^2) - \Big(\frac{1}{3}ad + \frac{1}{6}a^2\Big)\Big(\frac{1}{6}df^2 - \frac{1}{3}cdf - \frac{1}{3}c^2 d\Big) \\ &\quad + \frac{1}{3}ab(2c+f) + (2c+f)^2\Big(\frac{4}{90}a^2 d - \frac{8}{360}ad^2 - \frac{1}{60}a^3 - \frac{2}{30}a^2 d\Big). \end{aligned} \tag{22}$$

Noting the fourth-order conditions and ruling out $D$ in the truncation errors, one can arrive at

$$\begin{aligned} a &= \frac{1}{2} - \frac{1}{3(1-f^2)}, \\ b &= \frac{1}{36(1-f)(1+f)^2} - \frac{1}{48} - e, \end{aligned}$$

$$
\begin{aligned}
c &= \frac{1}{2}(1-f),\\
d &= \frac{1}{3(1-f^2)},\\
g &= \frac{e}{6(1+f)} - \frac{60(f-1)^2 - 27(1-f^2)^3}{25920(1-f^2)^3},
\end{aligned}
$$

with the coefficients of the truncation errors

$$
\begin{aligned}
\gamma_1 &= \frac{1}{4}e(f^2-1) - \frac{f}{144(1+f)^2} + \frac{1}{480},\\
\gamma_2 &= \frac{1-5f^2}{2880},\\
\gamma_3 &= \frac{1+2f-9f^2}{2160(1+f)^2}.
\end{aligned}
$$

Several types of algorithms are provided as follows:

**Case 1:** optimization of the norm $\gamma$ with respect to the two time coefficients $e$ and $f$. — The coefficients for the total minimization of $\gamma$ vs. the two time coefficients $e$ and $f$ are

$$
\begin{aligned}
\text{(B1)}\quad a &= 8.021956831035854\,\text{e–2}, & b &= 2.453837714743311\,\text{e–4},\\
c &= 2.731001965480090\,\text{e–1}, & d &= 4.197804316896410\,\text{e–1},\\
e &= 2.983541871380019\,\text{e–3}, & f &= 4.537996069039810\,\text{e–1},\\
g &= 4.432055863874196\,\text{e–6}.
\end{aligned}
\tag{23}
$$

In this case, the least norm $\gamma_{\min} \approx 1.57\,\text{e–5}$.

**Case 2:** optimization of the norm $\gamma$ with respect to one time coefficient. — For $f = 0.469$, the minimization of $\gamma$ with respect to the coefficient $e$, $\gamma_{\min} \approx 3.58\,\text{e–5}$, is presented when

$$
\begin{aligned}
\text{(B2)}\quad a &= 7.267093910261757\,\text{e–2}, & b &= 4.643903722145720\,\text{e–4},\\
c &= 0.2655\,\text{e+0}, & d &= 4.273290608973820\,\text{e–1},\\
e &= 2.943770559109599\,\text{e–3}, & g &= 4.848453347909131\,\text{e–7}.
\end{aligned}
\tag{24}
$$

If $e = 0.00295$, these coefficients of the form

$$
\begin{aligned}
\text{(B3)}\quad a &= 7.983881940379656\,\text{e–2}, & b &= 2.876347576330359\,\text{e–4},\\
c &= 2.727041225755580\,\text{e–1}, & d &= 4.201611805962030\,\text{e–1},\\
f &= 4.545917548488850\,\text{e–1}, & g &= 6.547567159073805\,\text{e–7}
\end{aligned}
\tag{25}
$$

lead to the minimization of $\gamma$ with respect to one parameter $f$, namely, $\gamma_{\min} \approx 1.70\,\text{e–5}$. On the other hand, at $e = 0$ the least norm is $\gamma_{\min} \approx 5.37\,\text{e–4}$ when

$$
\begin{aligned}
\text{(B4)}\quad a &= 2.983406822767010\,\text{e–2}, & b &= +4.617265851398423\,\text{e–3},\\
c &= 2.302638136341820\,\text{e–1}, & d &= +4.701659317723300\,\text{e–1},\\
f &= 5.394723727316360\,\text{e–1}, & g &= -3.360022691071039\,\text{e–4}.
\end{aligned}
\tag{26}
$$

**Case 3:** non-optimization. — At $b = 0$ and $e = 0$, we have $\gamma \approx 3.76\,\text{e–2}$ and

$$
\begin{aligned}
\text{(B5)}\quad a &= +6.756035959798290\,\text{e–1}, & c &= +1.35120719195966\,\text{e+0},\\
d &= -1.756035959798290\,\text{e–1}, & f &= -1.70241438391932\,\text{e+0},\\
g &= +3.513300435645027\,\text{e–3}.
\end{aligned}
\tag{27}
$$

If $e = 0.2$ and $f = 0.3$, we obtain $c = 0.35$, $\gamma \approx 4.47$ e–2 and

$$\begin{aligned} \text{(B6)} \quad a &= 1.33699633699634\,\text{e–1}, \qquad b = -1.973525406217710\,\text{e–1}, \\ d &= 3.66300366300366\,\text{e–1}, \qquad g = +2.517751328772039\,\text{e–2}. \end{aligned} \tag{28}$$

As stated above, the two types of new symplectic algorithms have been constructed by the operator $D$ associated with the third-order potential derivatives added to various compositions. It is expected that the norm $\gamma$ for each optimal method is much smaller than that of any algorithm without optimization. What about the numerical performance of these newly proposed methods in practical computations? Saying this in another way, it is strongly desired to know whether the symplectic integrators computed by the optimization of the norm are indeed better than those without the optimization. Numerical simulations will answer this question.

## 3 NUMERICAL EXPERIMENTS

Physical models we adopt are the Hénon-Heiles system and the Newtonian core-shell system with a quadrupole (Vieira & Letelier 1999). The newly proposed algorithms are independently applied to numerically solve the two problems. For comparison, the existing methods, the usual Forest-Ruth fourth-order non-gradient symplectic algorithm (18) and the Chin force gradient fourth-order symplectic scheme (19), are taken as reference integrators. Additionally, it is worth noting whether regular or chaotic orbits in the considered systems influence the effectiveness of these new algorithms.

### 3.1 Hénon-Heiles System

As a simplified galactic model, the Hénon-Heiles system is a Hamiltonian function given by

$$H = \frac{1}{2}(p_x^2 + p_y^2 + x^2 + y^2) + x^2 y - \frac{1}{3}y^3. \tag{29}$$

In this system, the kinetic energy

$$T = (p_x^2 + p_y^2)/2,$$

and the potential energy

$$V = (x^2 + y^2)/2 + x^2 y - y^3/3.$$

The related partial derivatives with respect to the potential are listed as follows:

$$\begin{aligned} \mathcal{B}_1(x,y) &= V_x = x(1+2y), \qquad \mathcal{B}_2(x,y) = V_y = x^2 + y - y^2; \\ V_{xx} &= 1 + 2y, \qquad V_{xy} = V_{yx} = 2x, \qquad V_{yy} = 1 - 2y; \\ V_{xxy} &= V_{xyx} = V_{yxx} = 2, \qquad V_{yyy} = -2, \end{aligned}$$

and $V_{ijk} \equiv 0$ for other cases, where indexes $i$, $j$ and $k$ range from 1 and 2, corresponding to $x$ and $y$ components respectively. The two components of the operator $C$ representing the momenta are expressed as

$$\begin{aligned} \mathcal{C}_1(x,y) &= Cp_x = 2\sum_{j=1}^{2} V_j V_{xj} = 2x[(1+2y)^2 + 2(x^2 + y - y^2)], \\ \mathcal{C}_2(x,y) &= Cp_y = 2\sum_{j=1}^{2} V_j V_{yj} = 2[2x^2(1+2y) + (x^2 + y - y^2)(1-2y)]. \end{aligned}$$

Moreover, the two components of the operator $D$ representing the momenta are

$$\begin{aligned}\mathcal{D}_1(x,y) &= Dp_x = -2\sum_{j=1}^{2}\sum_{k=1}^{2} V_k(2V_{jk}V_{xj} + V_jV_{xjk}) \\ &= -4x(1+2y)[(1+2y)^2 + 5x^2 + y - y^2] \\ &\quad -4x(x^2 + y - y^2)(5+2y), \\ \mathcal{D}_2(x,y) &= Dp_y = -2\sum_{j=1}^{2}\sum_{k=1}^{2} V_k(2V_{jk}V_{yj} + V_jV_{yjk}) \\ &= -4x^2(1+2y)(5+2y) - 4(x^2 + y - y^2) \\ &\quad \cdot[3x^2 + (1-2y)^2 - y + y^2].\end{aligned}$$

Hence, the difference schemes of the A type algorithms (5) from the $(n-1)$th step to the $n$th step read as

$$\text{(A)}\quad \begin{cases} x' = x_{(n-1)} + a\tau p_{x(n-1)}, \\ y' = y_{(n-1)} + a\tau p_{y(n-1)}; \\ p'_x = p_{x(n-1)} - b\tau\mathcal{B}_1(x',y') + c\tau^3\mathcal{C}_1(x',y'), \\ p'_y = p_{y(n-1)} - b\tau\mathcal{B}_2(x',y') + c\tau^3\mathcal{C}_2(x',y'); \\ x'' = x' + d\tau p'_x, \\ y'' = y' + d\tau p'_y; \\ p''_x = p'_x - e\tau\mathcal{B}_1(x'',y'') + f\tau^3\mathcal{C}_1(x'',y'') + g\tau^5\mathcal{D}_1(x'',y''), \\ p''_y = p'_y - e\tau\mathcal{B}_2(x'',y'') + f\tau^3\mathcal{C}_2(x'',y'') + g\tau^5\mathcal{D}_2(x'',y''); \\ x''' = x'' + d\tau p''_x, \\ y''' = y'' + d\tau p''_y; \\ p_{xn} = p''_x - b\tau\mathcal{B}_1(x''',y''') + c\tau^3\mathcal{C}_1(x''',y'''), \\ p_{yn} = p''_y - b\tau\mathcal{B}_2(x''',y''') + c\tau^3\mathcal{C}_2(x''',y'''); \\ x_n = x''' + a\tau p_{xn}, \\ y_n = y''' + a\tau p_{yn}. \end{cases} \tag{30}$$

In a similar way, the difference schemes of the B type algorithms (20) can also be given.

With the increase of energy $E$ as the perturbation of the system, the nonlinearity of the system becomes stronger and stronger. For energy $E = 1/7$, the main part of the phase space is chaotic, as described in the Poincaré section of Figure 1. This plot is drawn by the use of method A1 with a fixed step size of 0.1. The other methods give almost the same plot. In order to gain detailed insight into the effectiveness of the A type algorithms, Figure 2 draws relative energy errors $\Delta E/E$ for these schemes applied to an ordered orbit with initial conditions $x = 0.1$, $y = 0.2$ and $p_x = 0.25$. It can be seen clearly that the optimal methods A1–A4 are always better than the non-optimal methods A5 and A6 in terms of the numerical accuracy, and explicitly superior to the force gradient method Ch and the usual non-gradient symplectic algorithm FR. These conclusions are also applicable to the B type algorithms used to integrate a chaotic orbit with initial conditions $x = 0.1$, $y = 0.2$ and $p_x = 0.3$. See Table 1 for details.

Besides the energy accuracy, of course the position or momentum error can also be used as a criterion for evaluating the quality of each symplectic integrator. As shown in Figure 3, for some time any of the optimal methods A1, A2, A4 or B1–B3 has given much better results than the non-optimal methods A5, A6, B5, B6 or FR in terms of the accuracy of the position error $|\boldsymbol{\Delta r}|$ either

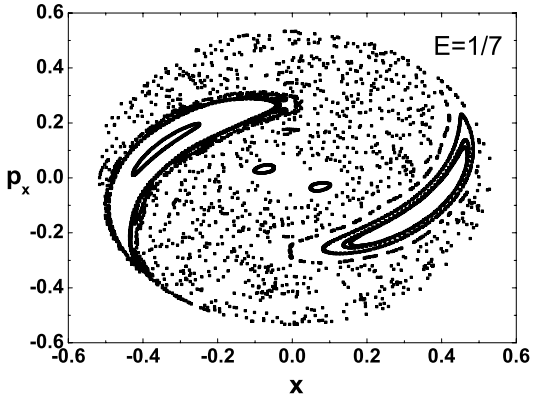


**Fig. 1** Poincaré section of the plane $y = 0$ and $p_y > 0$ for the Hénon-Heiles system.

**Table 1** Energy accuracy measured by $\max|\Delta E/E|$ during the integration time of 100 000 and the computational cost of each B type algorithm when solving a chaotic orbit of the Hénon-Heiles system, and using a fixed time step of $\tau = 0.1$.

| Algorithm | B1 | B2 | B3 | B4 | B5 | B6 | FR | Ch |
|---|---|---|---|---|---|---|---|---|
| Accuracy | 4.5 e–9 | 4.0 e–9 | 9.0 e–9 | 3.0 e–7 | 1.2 e–5 | 3.5 e–5 | 3.3 e–5 | 1.0 e–6 |
| CPU time (s) | 2 | 2 | 2 | 2 | 2 | 2 | 1 | 1 |

for the regular orbit or for the chaotic orbit. Methods A3 and Ch or B4 and Ch have almost the same accuracy, which is inferior to that of A1 but superior to that of FR. In short, the numerical performances in the position errors are basically in agreement with those of the energy accuracies. Here are two points to illustrate. One is the reference orbits which are obtained from a 12th-order Cowell integration scheme. The other is the evolution of the position errors with time, which would be unlike that of the energy errors. It is reasonable that the position errors of a symplectic integrator should grow exponentially with time for a chaotic orbit, but there is no drift in energy. It should be noted that this exponential growth cannot be permanent. In fact, there is no longer an increase of the position errors after the time when $|\boldsymbol{\Delta r}|$ is equal to one. This is due to the saturation of orbits in a bounded region. This similar case also occurs when the two-nearby-trajectories method is used to calculate Lyapunov exponents (Wu et al. 2006). Fortunately, renormalization can avoid the appearance of this problem in the computation of the Lyapunov exponents.

### 3.2 Newtonian Core-shell System with a Quadrupole

In the cylindrical coordinates $(\rho, \phi, z)$, the Newtonian core-shell model with a quadrupole (Vieira & Letelier 1999) is written as

$$H = \frac{1}{2}(p_\rho^2 + p_z^2) + \frac{1}{2}\frac{L^2}{\rho^2} - \frac{1}{R} + \frac{1}{2}\mathcal{Q}(2z^2 - \rho^2), \tag{31}$$

where $R = \sqrt{\rho^2 + z^2}$, $L$ is the constant magnitude of the angular momentum and $\mathcal{Q}$ stands for the quadrupole parameter.

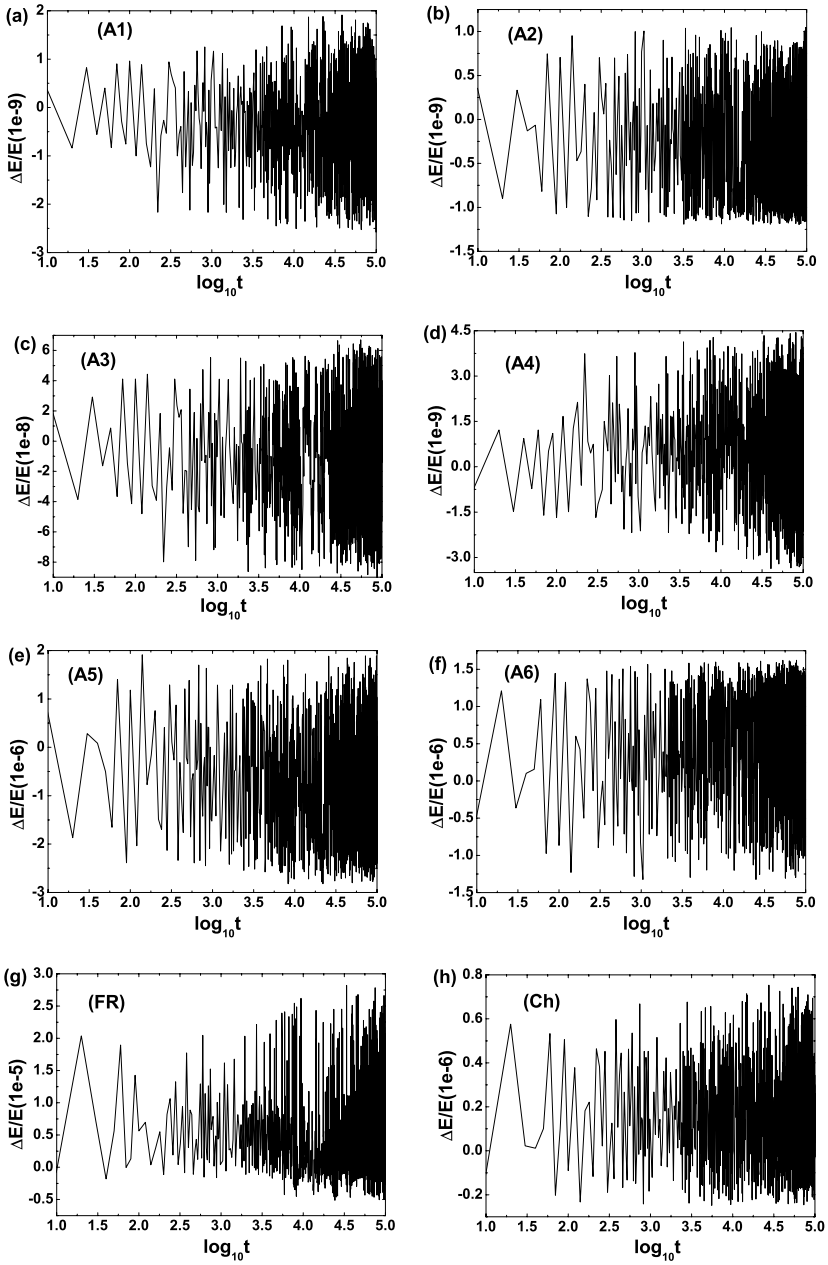


**Fig. 2** Relative energy error $\Delta E/E$ for each of the A type algorithms solving an ordered orbit with initial conditions $x = 0.1$, $y = 0.2$ and $p_x = 0.25$ in Fig. 1.

The quadrupolar shell plays an important role in providing a perturbative force. The larger the quadrupolar parameter becomes, the stronger the chaos is if energy $E$ and the angular momentum $L$ satisfy a certain condition in which chaos occurs. For example, a strong chaotic belt appears in Figure 4 when $E = -2.12 \times 10^{-2}$, $L = 3.8$ and $\mathcal{Q} = -1.2047 \times 10^{-5}$. Now, we employ a chaotic

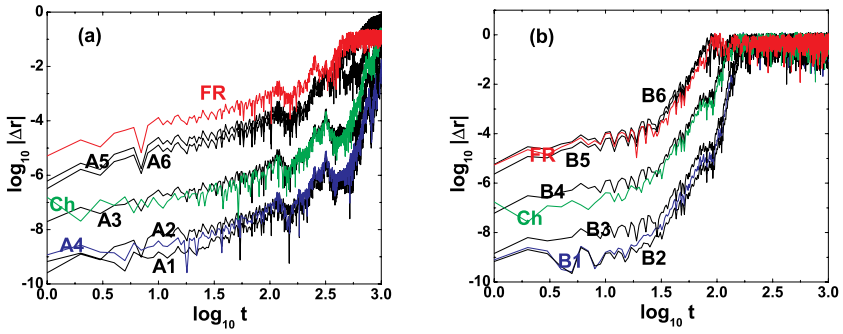


**Fig. 3** Evolution of the position error $\log_{10}|\boldsymbol{\Delta r}|$ with $\log_{10} t$. Panel (a) relates to the A type algorithms solving the ordered orbit of Fig. 2, and Panel (b) to the B type algorithms solving the chaotic orbit of Table 1.

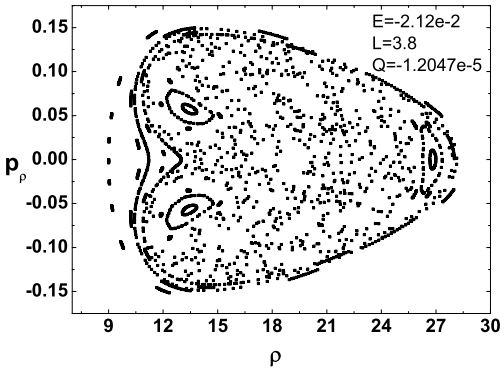


**Fig. 4** Poincaré section on the plane $z = 0$ and $p_z > 0$ for the Newtonian core-shell system.

orbit of initial conditions $\rho = 15$, $z = 5$ and $p_\rho = 0.1$ to check the numerical accuracy of the related methods with a step size of $\tau = 0.5$. As in Figure 2, the results in Figure 5 show that any of the optimal methods A1–A4 is still better than the other methods A5, A6, FR or Ch. If the chaotic orbit is replaced with an ordered orbit with initial conditions $\rho = 13$, $z = 5$ and $p_\rho = 0.1$ and the A type algorithms are replaced by the B type algorithms, Table 2 tells us similar results, that the optimal methods B1–B4 are superior to the non-optimal methods B5, B6, FR and Ch in terms of accuracy of energy calculations. On the other hand, Figure 6 also shows that the position errors of the optimal methods A1, A2, A4 and B1–B3 are the smallest, and that of the FR method is the largest. As a notable point, unlike Figure 3, Figure 6 shows no saturation of orbits during the considered time. In other words, the position errors for the core-shell problem grow much more slowly than ones for the Hénon-Heiles system. Therefore, the chaos in the core-shell system should become rather weak.

Generally speaking, both the A type optimal methods and the B type optimal methods are drastically improved in terms of accuracy compared with the non-optimal methods, as shown in the above numerical simulations. This benefits from the least norm of the truncation errors. In addition, the optimal method A1 (or B1) with respect to two time coefficients is very close to the optimized method A2 (or B2) with respect to one time coefficient, because there is not an explicit difference

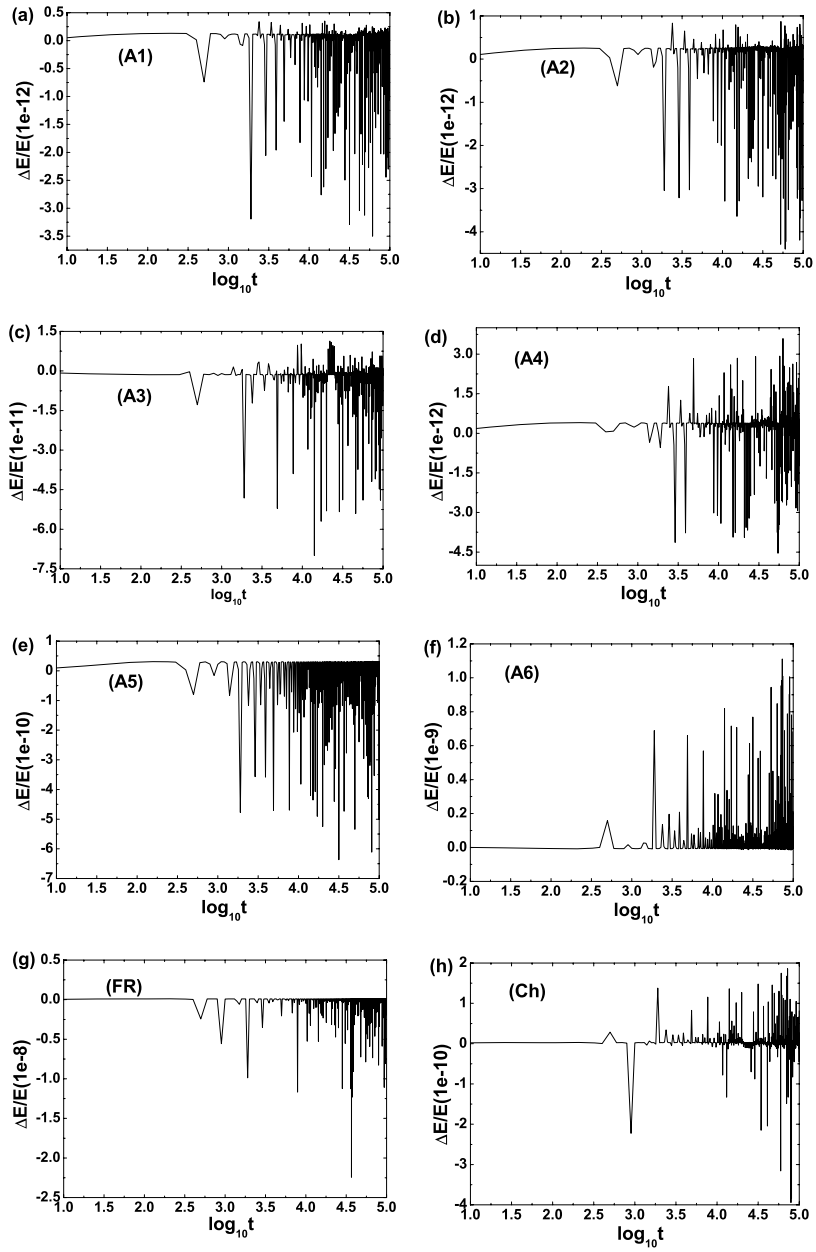


**Fig. 5** Relative energy error $\Delta E/E$ for each of the A type algorithms when solving a chaotic orbit with initial conditions $\rho = 15$, $z = 5$ and $p_\rho = 0.1$ in Fig. 4.

between the norm of the former and the one of the latter. In spite of these facts, we should emphasize that the least norm is merely a necessary but not sufficient condition for the minimum truncation errors. Obviously, the truncation errors depend on not only the three coefficients $\gamma_1$, $\gamma_2$ and $\gamma_3$ associated with the least norm, but also the commutators $[A,[A,[B,[A,B]]]]$, $[A,[A,[A,[A,B]]]]$ and $[B,[A,[A,[A,B]]]]$.

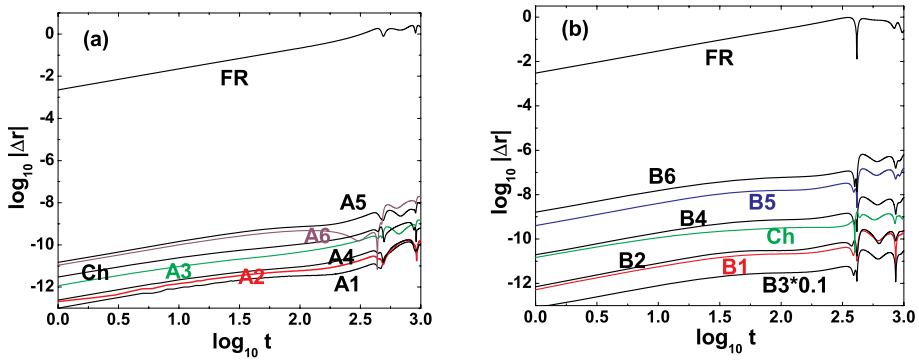


**Fig. 6** Evolution of the position error $\log_{10}|\boldsymbol{\Delta r}|$ with $\log_{10} t$. The left panel relates to the A type algorithms solving the chaotic orbit of Fig. 5, and the right panel to the B type algorithms solving the regular orbit of Table 2. Note that the symbol B3*0.1 means the plotted error $|\boldsymbol{\Delta r}|$ decreased by 10 times for the B3 method.

Finally, let us compare the computational cost among these methods. Each A type algorithm in Figure 2 needs about 2 s of CPU time, and in Figure 5 it uses about 4 s of CPU time. As to CPU time of the B type algorithms, we list them in Tables 1 and 2. It is shown obviously that the computational efficiency of the A type algorithms is faster than that of the B type algorithms. In addition, use of the operator $D$ leads to the A and B type algorithms having a little but not much additional computational cost, as compared with the usual non-gradient symplectic algorithm (18) of Forest & Ruth and the force gradient symplectic scheme (19) of Chin. In particular, an interesting result which can be seen from Tables 3 and 4 is that any A type algorithm is faster in the computations than the FR and Ch methods when they use smaller time steps to obtain nearly the same levels of energy accuracies given by algorithms like A1. It is more interesting to apply the same time steps to compare our methods with a 6th-order symplectic integrator S6 and an 8th-order symplectic integrator S8 of Yoshida (1990). In terms of accuracy, our optimal algorithms A1 and A2 are superior to S6, and even almost equivalent to S8. On the other hand, they are close to S6 in terms of computational cost.

**Table 2** Energy accuracy measured by $\max|\Delta E/E|$ during the integration time of 100 000 and the computational cost of each B type algorithm when solving an ordered orbit of the core-shell system, and using a fixed time step of $\tau = 0.5$.

| Algorithm | B1 | B2 | B3 | B4 | B5 | B6 | FR | Ch |
|---|---|---|---|---|---|---|---|---|
| Accuracy | 8.0 e–12 | 9.0 e–12 | 1.2 e–11 | 3.5 e–10 | 6.0 e–9 | 3.0 e–8 | 4.0 e–8 | 7.0 e–10 |
| CPU time (s) | 7 | 7 | 7 | 7 | 7 | 7 | 2 | 2 |

## 4 SUMMARY

With the help of both the operator $D$ associated with the third-order potential derivatives and the force gradient operator $C$ corresponding to the included second-order potential derivatives, we present new fourth-order explicit symplectic integrators for the natural splitting of a Hamiltonian into the kinetic and potential energies. Considering that the norm of the truncation errors is required to be minimized, we also give many optimal algorithms. It is argued through various numerical tests

**Table 3** Comparisons between the computational cost of the FR and Ch methods and that of the newly proposed methods when these algorithms use different time steps in solving the chaotic orbit of Table 1, and obtain the same levels of the energy accuracy. For an in-depth comparison, a 6th-order symplectic integrator S6 and an 8th-order symplectic integrator S8 of Yoshida with the same time step as the new schemes are also included, respectively.

| Algorithm | A1 | A2 | B1 | FR | Ch | S6 | S8 |
|---|---|---|---|---|---|---|---|
| Accuracy | 3.0 e–9 | 1.5 e–9 | 4.5 e–9 | 3.0 e–9 | 4.0 e–9 | 6.0 e–7 | 7 e–9 |
| Time step | 0.1 | 0.1 | 0.1 | 0.01 | 0.02 | 0.1 | 0.1 |
| CPU time (s) | 2 | 2 | 2 | 11 | 4 | 2 | 4 |

**Table 4** Same as Table 3 but the Ordered Orbit of Table 2 is Used

| Algorithm | A1 | A2 | B1 | FR | Ch | S6 | S8 |
|---|---|---|---|---|---|---|---|
| Accuracy | 5.0 e–12 | 6.0 e–12 | 8.0 e–12 | 3.0 e–12 | 1.0 e–12 | 3.5 e–11 | 2.8 e–13 |
| Time step | 0.5 | 0.5 | 0.5 | 0.05 | 0.1 | 0.5 | 0.5 |
| CPU time (s) | 4 | 4 | 7 | 17 | 6 | 4 | 9 |

that the optimal algorithms A1–A4 and B1–B4 have very good demonstrations of the accuracy of energy calculations. It can be concluded from the energy accuracy, the position accuracy and the computational efficiency that any of the optimized methods A1, A2 or A4 can be regarded as the best.

The new methods proposed are suitable for studying cosmological Hamiltonian evolution problems (Ma et al. 2009; Wu 2010) and gravitational few-body problems such as restricted three-body problems. In addition, higher-order symplectic algorithms can be given similarly in principle. It is worth emphasizing that an advantage of designing the symplectic schemes like the present treatment compared with the usual way lies in using fewer sub-steps or products of exponential functions on Lie operators. Of course, operators with higher-order potential derivatives, such as $[B,[A,[B,[A,[B,[A,B]]]]]]$ associated with fourth-order potential derivatives and $[B,[A,[B,[A,[B,[A,[B,[A,B]]]]]]]]$ corresponding to fifth-order potential derivatives, can also be added to these symmetric composition methods.

**Acknowledgements** It is a pleasure to thank the referee for valuable suggestions. This research is supported by the National Natural Science Foundation of China (Grant No. 10873007). It is also supported by the Science Foundation of Jiangxi Education Bureau (GJJ09072), and the Program for an Innovative Research Team of Nanchang University.

## References

Chambers, J. E., & Murison, M. A. 2000, AJ, 119, 425
Chin, S. A. 1997, Phys. Lett. A, 226, 344
Chin, S. A. 2007, Phys. Rev. E, 75, 036701
Feng, K. 1985, Proc. 1984 Beijing Symp. Diff. Geom. and Diff. Eq. (Beijing: Science Press)
Feng, K. 1986, J. Comput. Math., 4, 279
Forest, E., & Ruth, R. 1990, Physica D Nonlinear Phenomena, 43, 105
Li, R., & Wu, X. 2010a, Science China Physics, Mechanics & Astronomy, 53, 1600
Li, R., & Wu, X. 2010b, Acta. Phys. Sin., 59, 7135 (in Chinese)

Liao, X. H. 1997, Celest. Mech. Dyn. Astron., 66, 243
Lubich, C., Walther, B., & Brügmann, B. 2010, Phys. Rev. D, 81, 104025
Ma, D. Z., Wu, X., & Zhong, S. Y. 2008, ApJ, 687, 1294
Ma, D. Z., Wu, X., & Zhong, S. Y. 2009, RAA (Research in Astronomy and Astrophysics), 9, 1185
Omelyan, I. P., Mryglod, I. M., & Folk, R. 2002, Phys. Rev. E, 66, 026701
Preto, M., & Saha, P. 2009, ApJ, 703, 1743
Ruth, R. D. 1983, IEEE Trans. Nucl. Sci., 30, 2669
Vieira, W. M., & Letelier, P. S. 1999, ApJ, 513, 383
Wisdom, J., & Holman, M. 1991, AJ, 102, 1528
Wisdom, J., Holman, M., & Touma, J. 1996, Field Inst. Commun., 10, 217
Wu, X., Huang, T. Y., & Zhang, H. 2006, Phys. Rev. D, 74, 083001
Wu, X. 2010, RAA (Research in Astronomy and Astrophysics), 10, 211
Wu, X., Huang, T. Y., Wan, X. S., & Zhang, H. 2007, AJ, 133, 2643
Xu, J., & Wu, X. 2010, RAA (Research in Astronomy and Astrophysics), 10, 173
Yoshida, H. 1990, Phys. Lett. A, 150, 262
Zhong, S. Y., & Wu, X. 2010, Phys. Rev. D, 81, 104037
Zhong, S. Y., Wu, X., Liu, S. Q., & Deng, X. F. 2010, Phys. Rev. D, 82, 124040